Preparation and evaluation of novel pyrazolo[1,5-*a*]pyrimidine acetamides, closely related to DPA-714, as potent ligands for imaging the TSPO 18 kDa with PET

Vincent Médran-Navarrete, Annelaure Damont, Marie-Anne Peyronneau, Bertrand Kuhnast, Nicholas Bernards, Géraldine Pottier, Frank Marguet, Frédéric Puech, Raphaël Boisgard, Frédéric Dollé

PII: S0960-894X(14)00120-6
DOI: http://dx.doi.org/10.1016/j.bmcl.2014.01.080
Reference: BMCL 21315

To appear in: *Bioorganic & Medicinal Chemistry Letters*

Received Date: 29 August 2013
Revised Date: 24 January 2014
Accepted Date: 27 January 2014

Please cite this article as: Médran-Navarrete, V., Damont, A., Peyronneau, M-A., Kuhnast, B., Bernards, N., Pottier, G., Marguet, F., Puech, F., Boisgard, R., Dollé, F., Preparation and evaluation of novel pyrazolo[1,5-*a*]pyrimidine acetamides, closely related to DPA-714, as potent ligands for imaging the TSPO 18 kDa with PET, *Bioorganic & Medicinal Chemistry Letters* (2014), doi: http://dx.doi.org/10.1016/j.bmcl.2014.01.080

Preparation and evaluation of novel pyrazolo[1,5-*a*]pyrimidine acetamides, closely related to DPA-714, as potent ligands for imaging the TSPO 18 kDa with PET

Vincent Médran-Navarrete,[a] Annelaure Damont,[a] Marie-Anne Peyronneau,[a] Bertrand Kuhnast,[a] Nicholas Bernards,[a,b] Géraldine Pottier,[a,b] Frank Marguet,[c] Frédéric Puech,[c] Raphaël Boisgard,[a,b] Frédéric Dollé.[a]

[a] *CEA, I2BM, Service Hospitalier Frédéric Joliot, Orsay, France.*
[b] *Inserm, U1023, Université Paris Sud, Orsay, France*
[c] *Exploratory Unit, Sanofi, Chilly-Mazarin, France.*

ABSTRACT

A series of four novel analogues of DPA-714, bearing a fluoroalkynyl side chain (with a length ranging from three to six carbon atoms) in replacement of the fluoroethoxy motif, have been synthetized in six steps from commercially available methyl 4-iodobenzoate. The synthetic strategy for the preparation of these *N,N*-diethyl-2-(2-(4-(ω-fluoroalk-1-ynyl)phenyl)-5,7-dimethylpyrazolo[1,5-a]pyrimidin-3-yl)acetamides (**7a-d**) consisted in derivatizing a key iodinated building block featuring the pyrazolopyrimidine acetamide backbone of DPA-714, by Sonogashira couplings with various alkynyl reagents. The resulting alkynols were subsequently fluorinated, yielding the expected target derivatives. All four analogues exhibited slightly higher affinity and selectivity towards

the TSPO 18 kDa (K_i vs [^{3}H]PK11195 : 0.35-0.79 nM ; K_i vs [^{3}H]flunitrazepam : > 1000 nM) when compared to DPA-714 (K_i vs [^{3}H]PK11195 : 0.91 nM ; K_i vs [^{3}H]flunitrazepam : > 1000 nM). Lipophilicities (HPLC, $LogD_{7.4}$) increased with the chain length (from 3.6 to 4.3) and were significantly higher than the one determined for DPA-714 (2.9). Preliminary *in vitro* metabolism evaluation using rat microsomal incubations and LC-MS analyses showed, for all four novel analogues, the absence of defluorinated metabolites. Among them, the fluoropentynyl compound, DPA-C5yne (**7c**), was selected, labelled in one single step with fluorine-18 from the corresponding tosylate and *in vivo* evaluated with PET on our in-house-developed rat model of acute local neuroinflammation.

The translocator protein (TSPO 18 kDa), formerly known as the peripheral benzodiazepine receptor (PBR), is a highly lipophilic tryptophan-rich protein comprising 169 amino acids.[1-3] It is located in the outer mitochondrial membrane of cells where it combines with a 32 kDa voltage-dependent anion channel (VDAC) and a 30 kDa adenine nucleotide carrier (ANC).[3,4] This trimeric complex, involved in the mitochondrial permeability transition pore (MPTP), plays an important role in certain transport processes. For example, it is well-established that TSPO controls the translocation of cholesterol from the outer to inner mitochondrial membrane, where it is converted to pregnenolone, a key intermediate for the biosynthesis of steroids.[5] While it is minimally produced in the healthy brain,[6] the translocator protein is overexpressed in inflamed brains.[7-9] As a result, TSPO has become over the years an attractive biological target for imaging neuroinflammatory disorders, for example in Alzheimer's or Parkinson's disease, using PET.[10]

Regarding TSPO tracers, the first PET-radioligand synthesized, the isoquinoline carboxamide [^{11}C]PK11195 (Figure 1), has been used clinically since 1984.[11] Even though it is still considered as a standard, [^{11}C]PK11195 presents serious limitations for PET imaging such as a poor signal-to-noise ratio and low brain penetration as well as the short radioactive half-life of carbon-11 ($t_{1/2}$ = 20.4 min).[12] These drawbacks have encouraged the design of improved radiotracers.[13-18] For instance, in the phenoxyphenyl acetamide class, [^{11}C]DAA1106 was found to exhibit a higher specificity[19-21] and its fluorinated analogue, FEDAA1106, labelled with the longer half-lived positron-emitter fluorine-18 ($t_{1/2}$ = 109.8 min), turned out to be also a better radioligand, with a better signal-to-noise ratio compared to [^{11}C]PK11195.[22-23] [^{18}F]PBR06 is another representative of this series that has been labelled with introduction of the fluorine-18 at the *N*-acyl function.[24,25] Concomitantly, carbon-11 or fluorine-18-labelled compounds featuring a pyridine motif were developed. Among them, [^{11}C]PBR28, a ligand displaying encouraging *in vivo* imaging properties,[26-32] and the fluorinated analogues 6-[^{18}F]fluoro-PBR28 and [^{18}F]FEPPA, were reported in the literature.[33-35]

Another class of high affinity TSPO ligands gathers compounds related to the imidazopyridine alpidem[36] (Figure 1). A well-known fluorine-18-labelled example of this class is [^{18}F]PBR111.[37,38] Bioisosteric derivatives such as pyrazolopyrimidine acetamides have also been developed to target the TSPO. Within this sub-class, the best known compounds are [^{11}C]DPA-713[39-45] and [^{18}F]DPA-714[42,43,46-59] (Figure 1), both already *in vivo* evaluated at the preclinical and clinical stage. Even though [^{18}F]DPA-714 has a slightly higher lipophilicity than [^{11}C]DPA-713, which could lead to an increased non-specific binding, this radioactive compound allows longer imaging protocols and therefore can be considered as a more suitable radiotracer. The use of radioligands belonging to this class may also facilitate accurate quantitative interpretation of the PET data. Indeed, pyrazolopyrimidine acetamides show a relatively low difference in affinity (~ 4 fold) between the high- (HABs) and the low- or the mixed-affinity binders (LABs / MABs), when compared to the *N*-benzyl-*N*-(2-phenoxyaryl) acetamides PBR06 (~ 17 fold) or PBR28 (~ 50 fold).[60-62] Thus, the impact of inter-individual variations which are linked to the expression of different TSPO binding sites encoded by the rs6971 polymorphism at the gene level could be reduced, and may not require subject genotyping.

Recent studies clearly demonstrated [^{18}F]DPA-714 that rapidly and extensively undergoes *in vivo* metabolism in both rodents (rats) and non-human primates (baboons). In particular, the observed fluoroethoxy side chain cleavage leads to the formation of small radiometabolites entering the brain and lowering PET imaging quality and restraining quantitative analysis.[63,64] Regarding this metabolic pathway, we intended to improve DPA-714 stability by replacing the oxygen atom bridging the phenyl group and the fluoroethyl motif by a methylene unit. Such a modification gave rise to a new compound named CfO-DPA-714 whose corresponding fluorine-18-labelled version ([^{18}F]CfO-DPA-714, Figure 1) has recently been prepared and is currently evaluated *in vivo*.[65]

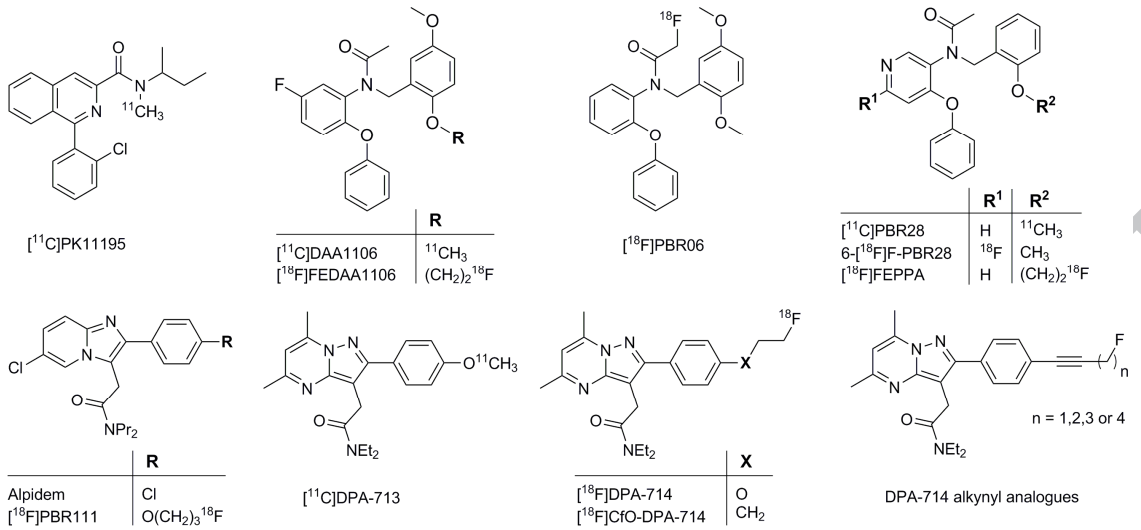

Figure 1. Selected TSPO ligands, including, at the right bottom corner, the general structure of the DPA-714 alkynyl analogues synthesized in the present work.

In this article, we report the chemical synthesis (Scheme 1 and Scheme 2) of a new subclass of DPA-714 analogues featuring an alkyne triple bond and a short alkane spacer linking the pyrazolopyrimidine scaffold and the fluorine atom (Figure 1). The series includes four compounds with a side chain ranging from three to six carbon atoms (**7a-d**). Preliminary evaluation of some of their physical and *in vitro* biological properties ($logD_{7.4}$, K_i against [^{3}H]PK11195 and [^{3}H]flunitrazepam) as well as *in vitro* metabolism studies for all four compounds are described. In addition, fluorine-18-labelling and first *in vivo* PET-imaging of one of them is also presented herein.

The synthesis of DPA-714 alkynyl analogues **7a-d** was envisaged from the key iodopyrazolopyrimidine **5** using the pathway depicted in Scheme 1.

Thus, the synthesis of compounds **7a-d** started with a nucleophilic addition of acetonitrile carbanion on the commercially available methyl 4-iodobenzoate **1,** leading to 3-oxopropanenitrile **2** upon the loss of the methoxide moiety. The reaction, initially performed with NaOMe in boiling acetonitrile,[39] was improved by using *n*-BuLi as a base at low temperature.[66] This strategy allowed to decrease ester hydrolysis and resulted in an improved reaction yield of 70 % compared to maximum 45% when using NaOMe. The resulting β-ketonitrile **2** was then *C*-alkylated with *N,N*-diethylchloroacetamide in presence of NaI in ethanolic sodium hydroxide. This reaction usually took a few days to reach completion and resulted in the formation of the expected *N,N*-diethylamide **3** with a modest yield of 40 %. In the next step, compound **3** was subjected to a first cyclization using monohydrated hydrazine in refluxing acetic acid to lead to the aminopyrazole **4** which was isolated in a moderate yield of 39 %. Finally, reaction of compound **4** with acetylacetone in boiling ethanol for 5 h allowed the pyrazolopyrimidine ring formation in 77% yield, and moreover in a clean and easy way since no side-product formation was observed. While cooling down the reaction mixture, the iodopyrazolopyrimidine **5** often crystallized in a pure form (shiny white solid) that did not require additional purification. In our synthesis strategy, compound **5** was a key intermediate since it could give access to a wide range of fluorinated alkynyl compounds in a straightforward (two steps) and versatile way. To generate the analogues **7a-d**, first Sonogashira couplings between **5** and the appropriate alkynyl alcohols were carried out to

give the alkynols **6a-d** in good to excellent yields (69 to 94 %). Then, compounds **6a-d** were submitted to fluorodeoxygenation using Deoxofluor® in methylene chloride to yield **7b-d** with variable efficiency (19 to 62 %). Typically, the reaction mixture was worked up after 48 h. For analogue **7b**, it is important not to run the reaction for too long otherwise a side-product involving allene formation is produced.

Finally, analogues **7b-d** were produced in six steps with chemical purities higher than 95 % (^{1}H NMR). Their structures were confirmed by ^{1}H NMR, ^{13}C NMR and MS (Table 1).[67]

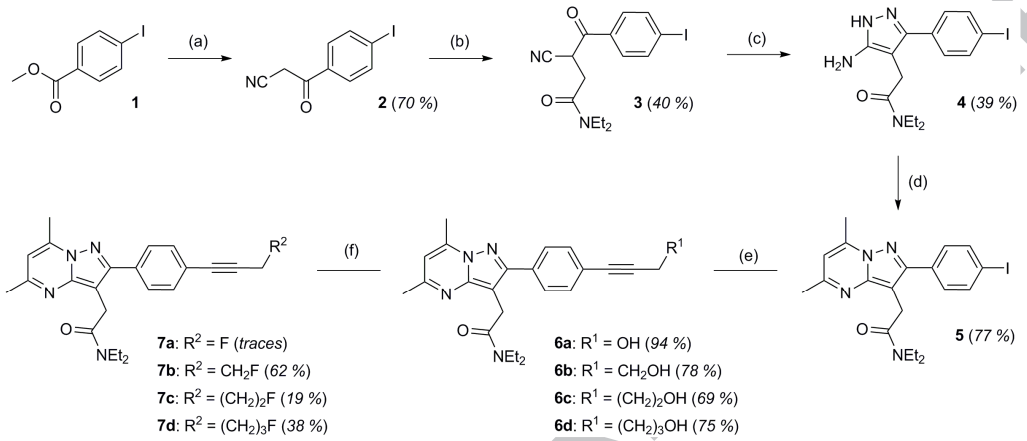

Scheme 1. Synthesis of the DPA-714 alkynyl analogues **7a-d**. Reagents and conditions: (a) *n*-BuLi, CH_3CN, THF, 30 min, -65 °C then methyl 4-iodobenzoate (**1**), 2 h, -65 °C to -45 °C; (b) NaOH, EtOH, 15 min then $ClCH_2C(O)NEt_2$, NaI, 4 days, r.t.; (c) $N_2H_4.H_2O$, AcOH, EtOH, 5-8 h, 80 °C; (d) acetylacetone, EtOH, 5 h, 80 °C; (e) alkynyl alcohol, CuI, $Pd(PPh_3)_2Cl_2$, Et_2NH, 24 h, r.t.; (f) Deoxofluor®, CH_2Cl_2, 2-4 days, r.t.

Regarding the analogue **7a**, since the fluorodeoxygenation turned out to be only partially successful when applied to alcohol **6a**, a different pathway was considered (Scheme 2). For the preparation of this compound (**7a**), the major improvement was made by performing the fluorination at the very beginning of the synthesis as depicted below (Scheme 2).

Thus, starting with the iodoester **1**, a Sonogashira coupling using 2-propyn-1-ol was first carried out to yield the propargylic alcohol **8** in 76 % yield. Then, **8** was submitted to fluorodeoxygenation using Deoxofluor® at room temperature in methylene chloride. Although this reaction was not clean (several by-products were observed on TLC), the fluoroester **9** was successfully isolated with a good purity in 30 % yield. The oxopropanenitrile **10** was then obtained in good to excellent yields (92 %) using similar conditions to those previously described. Analogously, *C*-alkylation with *N,N*-diethylchloroacetamide gave the amide **11** in a moderate 47 % yield. Cyclisation with hydrazine led to the aminopyrazole **12** in a moderate yield of 34 %, and was further converted to the pyrazolopyrimidine **7a** (81 % yield). Finally, the target fluoropropynyl compound **7a** was also obtained in six steps with a high purity and its structure was confirmed by ^{1}H NMR, ^{13}C NMR and MS (Table 1).[67]

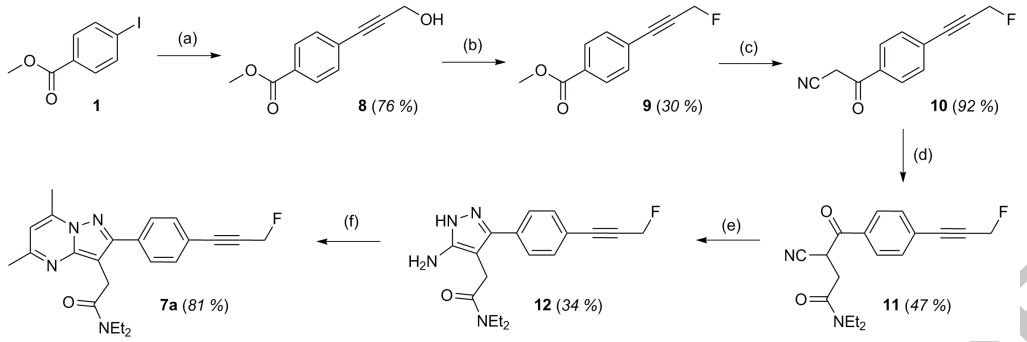

Scheme 2. Synthesis of the DPA-714 alkynyl analogue **7a**. Reagents and conditions: (a) 2-propyn-1-ol, CuI, $Pd(PPh_3)_2Cl_2$, Et_2NH, 24 h, r.t.; (b) Deoxofluor®, CH_2Cl_2, 2 days, r.t.; (c) *n*-BuLi, CH_3CN, THF, 30 min, -60 °C then compound **9**, 2 h, -60 °C; (d) NaOH, EtOH, 15 min then $ClCH_2C(O)NEt_2$, NaI, 4 days, r.t.; (e) $N_2H_4.H_2O$, AcOH, EtOH, 5 h, 80 °C; (f) acetylacetone, EtOH, 8 h, 80 °C.

Table 1
Analytical characterization (MS, ^1H NMR and ^{13}C NMR data) of DPA-714 fluoroalkynyl analogues **7a-d**.

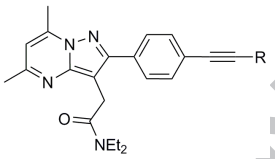

Compd	R	MW	m/z[a,b]	Fluoroalkynyl side chain ^1H NMR chemical shifts (δ, ppm, $CDCl_3$)[c,d]	Fluoroalkynyl side chain ^{13}C NMR chemical shifts (δ, ppm, $CDCl_3$)[c,d]
7a	CH_2-F	392	393	5.20 (d, 2H, J^2_{HF} = 47.6 Hz).	89.5 [d, J^3_{CF} = 12 Hz, C], 83.2 [d, J^2_{CF} = 22 Hz, C], 71.1 [d, J^1_{CF} = 164 Hz, CH_2].
7b	$(CH_2)_2$-F	406	407	4.60 (dt, 2H, J^2_{HF} = 46.8 Hz, J^3_{HH} = 6.8 Hz), 2.86 (dt, 2H, J^3_{HF} = 19.2 Hz, J^3_{HH} = 6.8 Hz).	89.4 [C], 85.1 [C], 81.3 [d, J^1_{CF} = 171 Hz, CH_2], 21.6 [d, J^2_{CF} = 24 Hz, CH_2].
7c	$(CH_2)_3$-F	420	421	4.62 (dt, 2H, J^2_{HF} = 47.2 Hz, J^3_{HH} = 6.0 Hz), 2.59 (t, 2H, *J* = 7.2 Hz), 2.01 (dq^5, 2H, J^3_{HF} = 25.6 Hz, J^3_{HH} = 6.0 Hz).	89.3 [C], 82.5 [d, J^1_{CF} = 164 Hz, CH_2], 81.2 [C], 29.5 [d, J^2_{CF} = 20 Hz, CH_2], 15.4 [d, J^3_{CF} = 4 Hz, CH_2].
7d	$(CH_2)_4$-F	434	435	4.52 (dt, 2H, J^2_{HF} = 47.2 Hz, J^3_{HH} = 6.0 Hz), 2.50 (t, 2H, *J* = 7.2 Hz), 1.89 (m, 2H), 1.75 (q^5, 2H, *J* = 7.2 Hz).	90.3 [C], 83.6 [d, J^1_{CF} = 164 Hz, CH_2], 81.1 [C], 29.5 [d, J^2_{CF} = 20 Hz, CH_2], 24.4 [d, J^3_{CF} = 5 Hz, CH_2], 19.1 [CH_2].

[a] ESI+ ionization ; [b] value corresponding to the $[M+H]^+$ peak; [c] Recorded on a 400 MHz Bruker Avance; [d] See note [67] in the "references and notes" section for a complete NMR description of compounds **7a-d**.

The $logD_{7.4}$ (*n*-octanol/buffer pH 7.4 partition coefficient) of compounds **7a-d** were evaluated on the basis of their HPLC retention times[68] and were also calculated using the ACD 11.0 software (Table 2). As expected, both measured and calculated $logD_{7.4}$ values where higher than those calculated for DPA-714, and increased as the fluorinated side chain R lengthened. Additionally, while analogues **7a** and **7b** exhibited comparable experimental $logD_{7.4}$ values, 3.61 and 3.67 respectively, **7c** and **7d** were found to be significantly more lipophilic with values slightly above 4.0.

The *in vitro* binding affinities of compounds **7a-d** for the TSPO 18 kDa were determined by competition with [^{3}H]PK11195 using membrane homogenates from rat heart. All four analogues exhibited high affinities for the protein with subnanomolar K_i values - all lower than the one measured for DPA-714 in the same assays - ranging from 0.35 nM (**7c**) to 0.79 nM (**7d**), as well as high specificity since no affinity for the central benzodiazepine receptor (CBR) was observed (Table 2).

Table 2
Lipophilicities and binding affinities of the DPA-714 fluoroalkynyl analogues **7a-d**.

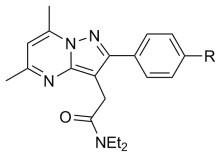

Compd	R	HPLC t_R (min)[a]	$logD_{7.4}$[b]	$clogD_{7.4}$[c]	Ki (TSPO) (nM)[d]	Ki (CBR) (nM)[e]
DPA-714	O-$(CH_2)_2$-F	1.10	2.89	3.21	0.91	> 1000
7a	C≡C-CH_2-F	1.19	3.61	3.81	0.54	> 1000
7b	C≡C-$(CH_2)_2$-F	1.20	3.67	4.19	0.74	> 1000
7c	C≡C-$(CH_2)_3$-F	1.30	4.06	4.58	0.35	> 1000
7d	C≡C-$(CH_2)_4$-F	1.33	4.35	5.03	0.79	> 1000

[a] HPLC conditions: UPLC/SQD Acquity BEH C18 column, 2.1 x 50 mm, 1.7 µm, mobile phase : H_2O (A) / CH_3CN + 0.1 % formic acid (B), gradient: 2 to 100 % (B) in 3 min, 1.0 mL/min; [b] See note [68] in the "references and notes" section for description of the $logD_{7.4}$ determination method using HPLC. [c] Calculated with ACD 11.0 software. [d] K_i values were determined using membrane homogenates from rat heart and screened against [^{3}H]PK11195 (K_d = 1.8 nM, C = 0.2 nM); [e] K_i values were determined using membrane homogenates from rat cerebral cortex and screened against [^{3}H]flunitrazepam (K_d = 2.1 nM, C = 0.4 nM).

Table 3
Microsomal metabolites of the DPA-714 fluoroalkynyl analogues **7a-d** (LC-MS and MS-MS analyses).

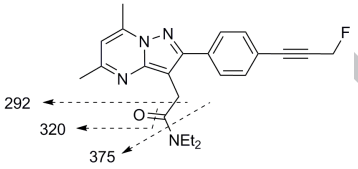

7a (*m/z 392*)

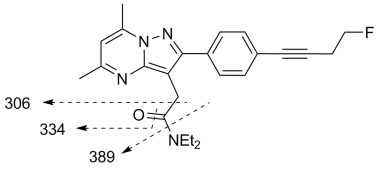

7b (*m/z 406*)

Compounds	t_R (min)[a]	$[M+H]^+$	Fragments[b]	t_R (min)[a]	$[M+H]^+$	Fragments[b]
Parent	15.66	393	375, 346, 320, 292	15.81	407	389, 360, 334, 306
M1	11.41	365 (–28)	347, 320, 292	11.68	379 (–28)	361, 334, 306
M2	11.0	409 (+16)	391, 362, 336, 308	11.19	423 (+16)	405, 376, 350, 322
M3	-	-	-	10.01	423 (+16)	405, 376, 350, 322
M4	-	-	-	5.89	439 (+32)	421, 392, 366, 338

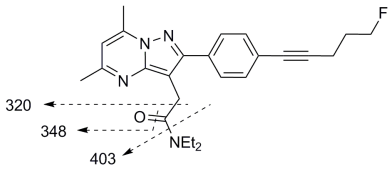

7c (*m/z 420*)

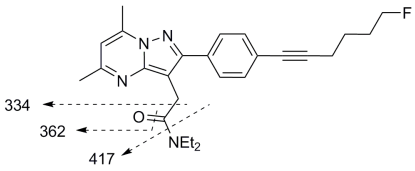

7d (*m/z 434*)

Compounds	t_R (min)[a]	$[M+H]^+$	Fragments[b]	t_R (min)[a]	$[M+H]^+$	Fragments[b]
Parent	17.05	421	403, 348, 320	15.81	435	417, 362, 334
M1	12.08	393 (–28)	375, 348, 320	11.68	407 (–28)	362, 334, 306
M2	11.37	437 (+16)	419, 364, 336	11.19	451 (+16)	433, 404, 378, 350
M3	8.92	437 (+16)	419, 364, 336	10.01	451 (+16)	433, 404, 378, 350
M4	3.43	453 (+32)	435, 380, 353	5.89	467 (+32)	449, 420, 394, 366

[a] HPLC conditions: Atlantis C18 column, 2.1 x 150 mm, 5 µm, mobile phase : H_2O + 0.05% formic acid (A) / CH_3CN + 0.05% formic acid (B), gradient (A / B) : 60:40 to 20:80 (20 min), 200 µL/min, detection at 275 nm. [b] See reference [69] in the "references and notes" section for a complete description of the materials and methods used for ESI-MS-MS analyses.

The metabolism of the four novel DPA-714 fluoroalkynyl analogues (**7a-d**) was also studied *in vitro* in rat liver microsomes.[69] Liquid chromatography-mass spectrometry (LC-MS and MS-MS) analyses, after 30 minutes of incubation, allowed the detection of the main metabolites formed for each analogue. The formation of two to four metabolites (M1 to M4) was observed as summarized in **Table 3**. For all four analogues **7a-d**, no metabolites resulting from the loss of the fluorine atom by cleavage of the fluoroalkynyl side chain was observed by LC-MS. The predominant metabolites, detected by HPLC at 275 nm and characterised by ESI-MS-MS analyses according to their fragmentation profiles, resulted from *N*-deethylation (M1, –28 Da) at the diethylacetamide position and also from hydroxylation (M2 and M3, +16 Da) or dihydroxylation (M4, +32 Da) most probably on the methyl groups of the pyrazolo-pyrimidine part of the molecule as already observed for DPA-714.[69]

The fluoropentynyl analogue **7c** (coded DPA-C5yne), displaying the highest TSPO binding affinity and a favourable *in vitro* metabolic profile, was chosen for radiofluorination[70,71] and first *in vivo* evaluation as potential PET imaging tool. Indeed, despite the good *in vitro* profile of the fluoropropynyl analogue **7a** that features an improved TSPO affinity in comparison to DPA-714, a better lipophilicity value than **7c** and only two main *in vitro* metabolites after 30 minutes microsomal incubation, compound **7c** was preferred based on i) the difficulties encountered to generate the corresponding precursor for labelling (tosyloxy derivative of **6a**) and ii) our past experience with compounds bearing comparable motif, e.g. the predicted issues to get efficient radiolabelling. Thus, the tosylate **13** was prepared from the alkynol **6c** by treatment with *p*-toluenesulfonic anhydride in dichloromethane in the presence of TEA at room temperature for 2-3 days, and obtained in 54% yield. Fluorine-18-labelling was then performed in a single-step procedure by nucleophilic aliphatic substitution using the activated K[^{18}F]F-Kryptofix K_{222} complex as the fluorinating reactant, in DMSO and heating at 100°C for 10 minutes[72] on a TRACERLab FX N Pro synthesizer (GEMS). Ready-to-inject **7c** (> 99% chemically and radiochemically pure, 55 to 110 GBq/µmol) was obtained in 20-25% decay-corrected yields (based on starting [^{18}F]fluoride) and within 50-60 min, semi-preparative HPLC purification and SepPak® Plus-based formulation included.

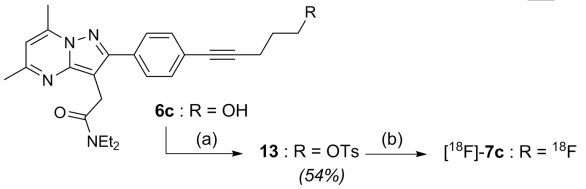

Scheme 3. Synthesis of the labelling precursor **13** and radioligand [^{18}F]-**7c**. Reagents and conditions: (a) Ts_2O, CH_2Cl_2, TEA, r.t., 3h; (b) i) K[^{18}F]F-K_{222}, K_2CO_3, DMSO, 100°C, 10 min, ii) cartridge purification (SepPak® Alumina N ™), iii) HPLC purification (Waters Symmetry® C-18).

First imaging properties of [^{18}F]DPA-C5yne ([^{18}F]-**7c**) were investigated *in vivo* with PET (INVEON PET/CT and PET only tomographes, Siemens) and compared to [^{18}F]DPA-714 on our in-house-developed rat model of acute local neuroinflammation. MicroPET studies were performed on anesthetized brain-lesioned Wistar rats 7 days after AMPA injection in their right striatum.[73] As shown in Figure 2A, the lesion (indicated by the white cross-cursor) could clearly be identified within the rat's brain from 5 minutes post-*i.v.*-injection of [^{18}F]-**7c** until the end of the PET acquisition. A relatively high contrast between the lesioned area and the corresponding area in the intact contralateral hemisphere was also observed. Uptake of [^{18}F]-**7c** in the lesioned striatum was high (0.24 percent of injected dose per milliliter (% ID/mL) at 60 min, Figure 2B) but slightly lower than the one routinely observed for [^{18}F]DPA-714 (0.30 % ID/mL, same time). Uptake of [^{18}F]-**7c** in the contralateral side was also significantly lower (0.05 % ID/mL at 60 min) than the one reported for [^{18}F]DPA-714 (0.08 % ID/mL at 60 min, respectively). Thus, an *in vivo* ipsilateral-to-contralateral ratio of 4.62 ± 0.4 ($p < 0.0001$), calculated as the bound tracer in the lesion versus the bound tracer in the contralateral side at 60 minutes post-injection, was found for [^{18}F]-**7c**, a notably higher value than the one measured for [^{18}F]DPA-714 (3.71 ± 0.4 ($p < 0.001$) or [^{11}C]PK11195 (1.65 ± 0.2 ($p < 0.001$), data not shown).

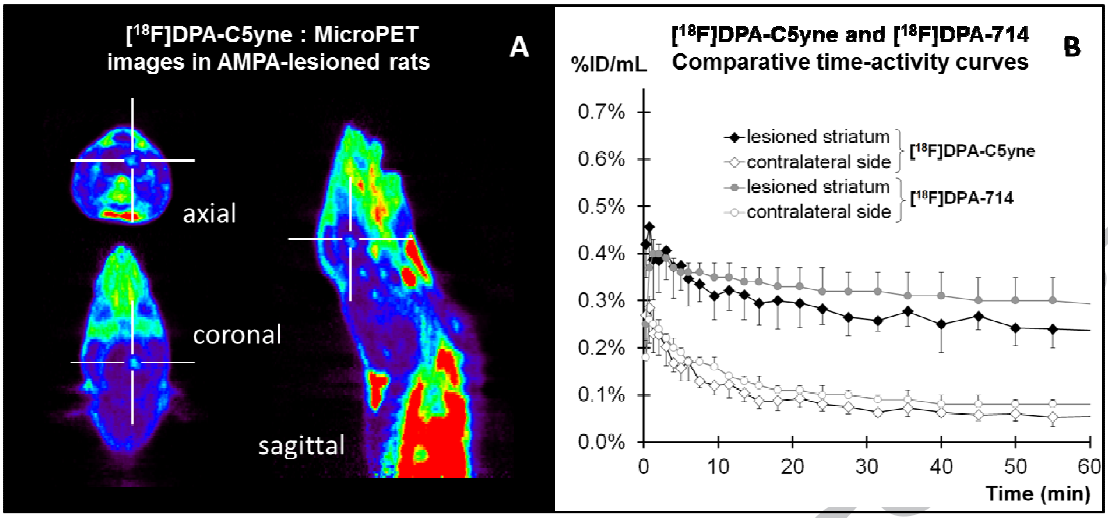

Figure 2. (**A**) MicroPET axial, coronal and sagittal summed images (5 - 60 minutes) following *i.v.* injection of [^{18}F]DPA-C5yne ([^{18}F]-**7c**) in AMPA-lesioned rat. A cross-cursor indicates in each section the visible right-side lesion. (**B**) Comparative time-activity curves expressed in between [^{18}F]DPA-C5yne ([^{18}F]-**7c**) and [^{18}F]DPA-714. Data are expressed in percent of injected dose per milliliter (% ID/mL) versus minutes (min).

Four novel closely related analogues of DPA-714 (**7a-d**) featuring a fluoroalkynyl side chain in replacement of the fluoroethoxy motif, have been synthetized in six steps from commercially available methyl 4-iodobenzoate. All target derivatives showed a high affinity and specificity toward the TSPO 18 kDa (as the parent molecule DPA-714). These compounds (**7a-d**) exhibited rather high lipophilicities compared to DPA-714, which nevertheless, keeps in the range favored for good passive cerebral penetration. Preliminary *in vitro* metabolism evaluation using rat microsomal incubations and LC-MS analyses have confirmed, for all derivatives, the stability of the chosen fluorination position, i.e. the alkynyl side chain. This results portend, in contrast to [^{18}F]DPA-714, the absence *in vivo* of small interfering radiofluorinated metabolites formation. Among the four analogues prepared, the fluoropentynyl compound **7c** was successfully labelled with fluorine-18 and its subsequent first PET *in vivo* evaluation has demonstrated its potential to image the TSPO 18 kDa. Additional studies, including *in vivo* metabolism analysis, in acute and chronic models of neurodegeneration will be performed in order to further evaluate the potential of this radioligand as a biomarker of neuroinflammation in neuropathological conditions.

Aknowledgements

The authors wish to thank LGCR Analytical Sciences (Sanofi, Chilly Mazarin) for logD measurements, Cyrielle Letaillandier for her technical assistance as well as Dr Dirk Roeda for proof reading the manuscript and suggesting linguistic corrections. This work was supported by CEA-I^{2}BM intramural programs, as well as the European Union's Seventh Framework Programme [FP7/2007-2013] INMiND (Grant agreement n° HEALTH-F2-2011-278850). PhD students Vincent Médran-Navarrete and Nicholas Bernards were in part supported by a CEA Irtelis doctoral grant and the EU FP7 INMiND program (see above), respectively.

References and notes

1. Beurdeley-Thomas, A.; Miccoli, L.; Oudard, S.; Dutrillaux, B.; Poupon, M. F. *J. Neurooncol.* **2000**, *46*, 45.
2. Joseph-Liauzun, E.; Delmas, P.; Shire, D.; Ferrara, P. *J. Biol. Chem.* **1998**, *273*, 2146.
3. Papadopoulos, V.; Baraldi, M.; Guilarte, T. R.; Knudsen, T. B.; Lacapere, J.-J.; Lindemann, P.; Norenberg, M. D.; Nutt, D.; Weizman, A.; Zhang, M.-R.; Gavish, M. *Trends Pharmacol. Sci.* **2006**, *27*, 402.
4. Casellas, P.; Galiegue, S.; Basile, A. S. *Neurochem. Int*. **2002**, *40*, 475.
5. Papadopoulos, V.; Brown, A. S. *J. Steroid Biochem. Mol. Biol*. **1995**, *53*, 103.
6. Gavish, M.; Bachman, I.; Shoukrun, R.; Katz, Y.; Veenman, L.; Weisinger, G.; Weizman, A. *Pharmacol. Rev*. **1999**, *51*, 629.
7. Bourguignon, J. J. in *Endogenous and synthetic ligands of mitochondrial benzodiazepine receptors: structure-affinity relationships, Peripheral Benzodiazepine Receptors* (Ed., E. Giensen-Crouse), Academic Press, London, **1993**, 59-85.
8. Kettenmann, H.; Burton, G. A.; Moenning, U. J. in *Neuroinflammation - from Bench to Bedside* (Ed.: Ernst Schering Research Foundation), Springer, Berlin, Heidelberg, **2002**, 1-234.
9. Raghavendra Rao, V. L.; Dogan, A.; Bowen, K. K.; Dempsey, R. J. *Exp. Neurol*. **2000**, *161*, 102.
10. Rupprecht, R.; Papadopoulos, V.; Rammes, G.; Baghai, T. C.; Fan, J.; Akula, N.; Groyer, G.; Adams, D.; Schumacher, M. *Nat. Rev. Drug Discovery* **2010**, *9*, 971.
11. Camsonne, R.; Crouzel, C.; Comar, D.; Mazière, M.; Prenant, C.; Sastre, J.; Moulin, M. A.; Syrota, A. *J. Labelled Compd. Radiopharm*. **1984**, *21*, 985.
12. Banati, R. B.; Newcombe, J.; Gunn, R. N. ; Cagnin, A.; Turkheimer, F.; Heppner, F.; Price, G.; Wegner, F.; Giovannoni, G.; Miller, D. H.; Perkin, D. G.; Smith, T.; Hewson, A. K.; Bydder, G.; Kreutzberg, G. W.; Jones, T.; Cuzner, M. L.; Myers, R. *Brain* **2000**, *123*, 2321.
13. Chauveau, F.; Boutin, H.; Van Camp, N.; Dollé, F.; Tavitian, B. *Eur. J. Nucl. Med. Mol. Imaging.* **2008**, *35*, 2304.
14. Dollé, F.; Luus, C.; Reynolds, A.; Kassiou, M. *Curr. Med. Chem.* **2009**, *16*, 2899.
15. Luus, C.; Hanani, R.; Reynolds, A.; Kassiou, M. *J. Labelled Compd. Radiopharm.* **2010**, *53*, 501.
16. Scarf, A. M.; Kassiou, M. *J. Nucl. Med.* **2011**, *52*, 677.
17. Roeda, D.; Kuhnast, B.; Damont, A.; Dollé, F. *J. Fluor. Chem.* **2012**, *134*, 107.
18. Ching, A. S. C.; Kuhnast, B.; Damont, A.; Roeda, D.; Tavitian, B.; Dollé, F. *Insights into Imaging* **2012**, *3*, 111.
19. Maeda, J.; Suhara, T.; Zhang, M. R.; Okauki, T.; Yasuno, F.; Ikoma, Y.; Inaji, M.; Nagai, Y.; Takano, A.; Obayashi, S.; Suzuki, K. *Synapse* **2004**, *52*, 283.
20. Chaki, S.; Funakoshi, T.; Yoshikawa, R.; Okuyama, S.; Okubo, T.; Nakazato, A.; Nagamine, M.; Tomisawa, K. *Eur. J. Pharmacol*. **1999**, *371*, 197.
21. Zhang, M. R.; Kida, T.; Noguchi, J.; Furutsuka, K.; Maeda, J.; Suhara, T.; Suzuki, K. *Nucl. Med. Biol.* **2003**, *30*, 513.
22. Fujimura, Y.; Ikoma, Y.; Yasuno, F.; Suhara, T.; Ota, M.; Matsumoto, R.; Nozaki, S.; Takano, A.; Kosaka, J.; Zhang, M. R.; Nakao, R.; Suzuki, K.; Kato, N.; Ito, H. *J. Nucl. Med.* **2006**, *47*, 43.
23. Zhang, M. R.; Maeda, J.; Ogawa, M.; Noguchi, J.; Ito, T.; Yoshida, Y.; Okauchi, T.; Obayashi, S.; Suhara, T.; Suzuki, K. *J. Med. Chem*. **2004**, *47*, 228.
24. Briard, E.; Shah, J.; Musachio, J. L.; Zoghbi, S. S.; Fujita, M.; Imaizumi, M.; Cropley, V.; Innis, R. B.; Pike, V. W. *J. Labelled Compd. Radiopharm.* **2005**, *48*, S4.
25. Briard, E.; Zoghbi, S.S.; Simeon, F. G.; Imaizumi, M.; Gourley, J. P.; Shetty, H. U.; Lu, S. Y.; Fujita, M.; Innis, R. B.; Pike, V. W. *J. Med. Chem.* **2009**, *52*, 688.
26. Briard, E.; Hong, J.; Musachio, J. L.; Zoghbi, S. S.; Fujita, M.; Imaizumi, M.; Cropley, V.; Innis, R. B., Pike, V. W. *J. Labelled Compd. Radiopharm.* **2005**, *48*, S71.
27. Imaizumi, M.; Kim, H.-J.; Zoghbi, S. S.; Briard, E.; Hong, J.; Musachio, J. L.; Ruetzler, C.; Chuang, D. M.; Pike, V. W.; Innis, R. B.; Fujita, M. *Neurosci. Lett*. **2007**, *411*, 200.
28. Brown, A. K.; Fujita, M.; Fujimura, Y.; Liow, J.-S.; Stabin, M.; Ryu, Y. H.; Imaizumi, M.; Hong, J.; Pike, V. W.; Innis, R. B. *J. Nucl. Med.* **2007**, *48*, 2072.

29. Briard, E.; Zoghbi, S. S.; Imaizumi, M.; Gourley, J. P.; Hong, J.; Cropley, V.; Fujita, M.; Innis, R. B.; Pike, V. W. *J. Med. Chem.* **2008**, *51*, 17.
30. Imaizumi, M.; Briard, E.; Zoghbi, S. S.; Gourley, J. P.; Hong, J.; Fujimura, Y.; Pike, V. W.; Innis, R. B.; Fujita, M. *NeuroImage* **2008**, *39*, 1289.
31. Fujita, M.; Imaizumi, M.; Zoghbi, S. S.; Fujimura, Y.; Farris, A. G.; Suhara, T.; Hong, J.; Pike, V. W.; Innis, R. B. *NeuroImage* **2008**, *40*, 43.
32. Kreisl, W. C.; Fujita, M.; Fujimura, Y.; Kimura, N.; Jenko, K. J.; Kannan, P.; Hong, J.; Morse, C. L.; Zoghbi, S. S.; Gladding, R. L.; Jacobson, S.; Oh, U.; Pike, V. W.; Innis, R. B. *NeuroImage* **2010**, *49*, 2924.
33. Damont, A.; Boisgard, R.; Kuhnast, B.; Lemée, F.; Raggiri, G.; Scarf, A. M.; Da Pozzo, E.; Selleri, S.; Martini, C.; Tavitian, B.; Kassiou, M.; Dollé, F. *Bioorg. Med. Chem. Lett.* **2011**, *21*, 4819.
34. Wilson, A. A.; Garcia, A.; Parkes, J.; McCormick , P.; Stephenson, K. A.; Houle, S.; Vasdev, N. *Nucl. Med. Biol.* **2008**, *35*, 305.
35. Mizrahi, R.; Rusjan, P. M.; Vitcu, I.; Ng, A.; Wilson, A. A.; Houle, S.; Bloomfield, P. M. *Mol. Imaging Biol.* **2013**, *15*, 353.
36. Selleri, S.; Bruni, F.; Costagli, C.; Costanzo, A.; Guerrini, G.; Ciciani, G.; Costa, B.; Martini, C. *Bioorg. Med. Chem.* **2001**, *9*, 2661.
37. Fookes, C. J. R.; Pham, T. Q.; Mattner, F.; Greguric, I.; Loc'h, C.; Liu, X.; Berghofer, P.; Shepherd, R.; Grégoire, M.-C.; Katsifis, A. *J. Med. Chem.* **2008**, *51*, 3700.
38. Dollé, F.; Hinnen, F.; Damont, A.; Kuhnast, B.; Fookes, C.; Pham, T.; Tavitian, B.; Katsifis, A. *J. Labelled Compd. Radiopharm.* **2008**, *51*, 435.
39. James, M. L.; Fulton, R. R.; Henderson, D. J.; Eberl, S.; Meikle, S. R.; Thomson, R.; Allan, D.; Dollé, F.; Fulhma, M. J.; Kassiou, M. *Bioorg. Med. Chem.* **2005**, *13*, 6188.
40. Thominiaux, C.; Dollé, F.; James, M.; Bramoullé, Y.; Boutin, H.; Besret, L.; Grégoire, M.-C.; Valette, H.; Bottlaender, M.; Tavitian, B.; Hantraye, P.; Selleri, S.; Kassiou, M. *Appl. Radiat. Isot.* **2006**, *64*, 570.
41. Boutin, H.; Chauveau, F.; Thominiaux, C.; Kuhnast, B.; Grégoire, M.-C.; James, M.; Jan, S.; Brulon, V.; Fontyn, Y.; Selleri, S.; Trébossen, R.; Hantraye, P.; Dollé, F.; Tavitian, B.; Kassiou, M. *J. Nucl. Med.* **2007**, *48*, 573.
42. Doorduin, J.; Klein, H. C.; Dierckx, R. A.; James, M.; Kassiou, M.; de Vries, E. F. J. *Mol. Imag. Biol.* **2009**, 11, 386.
43. Chauveau, F.; Van Camp, N.; Dollé, F.; Kuhnast, B.; Hinnen, F.; Damont, A.; Boutin, H.; James, M. L.; Kassiou, M.; Tavitian, B. *J. Nucl. Med.* **2009**, *50*, 468.
44. Leaver, K. R.; Reynolds, A.; Bodard, S.; Guilloteau, D.; Chalon, S.; Kassiou, M. *ACS Chemical Neuroscience* **2012**, *3*, 114.
45. Endres, C. J.; Coughlin, J. M.; Gage, K. L.; Watkins, C. C.; Kassiou, M.; Pomper, M. G. *J. Nucl. Med.* **2012**, *53*, 330.
46. James, M. L.; Fulton, R. R.; Vercouillie, J.; Henderson, D. J.; Garreau, L.; Chalon, S.; Dollé, F.; Costa, B.; Guilloteau, D.; Kassiou. M. *J. Nucl. Med.* **2008**, 49, 814.
47. Damont, A.; Hinnen, F.; Kuhnast, B.; Schollhorn-Peyronneau, M. A.; James, M. L.; Luus, C.; Tavitian, B.; Kassiou, M.; Dollé, F. *J. Labelled Compd. Radiopharm.* **2008**, *51*, 286.
48. Fookes, C.; Pham, T.; Mattner, F.; Greguric, I.; Loc'h, C.; Liu, X.; Berghofer, P.; Shepherd, R.; Grégoire, M. C.; Katsifis, A. *J. Med. Chem.* **2008**, *51*, 3700.
49. Martin, A.; Boisgard, R.; Theze, B.; Van Camp, N.; Kuhnast, B.; Damont, A.; Kassiou, M.; Dollé, F.; Tavitian, B. *J. Cereb. Blood Flow Metab.* **2010**, *30*, 230.
50. Martin, A.; Boisgard, R.; Kassiou, M.; Dollé F.; Tavitian, B. *Mol. Imag. Biol.* **2011**, 13, 10.
51. Zheng, J.; Boisgard, R.; Siquier-Pernet, K.; Decaudin, D.; Dollé, F.; Tavitian, B. *Mol. Pharmaceutics* **2011**, *8*, 823.
52. Winkeler, A.; Boisgard, R.; Awde, A. R.; Dubois, A.; Thézé, B.; Zheng, J.; Ciobanu, L.; Dollé, F.; Viel, T.; Jacobs, A. H.; Tavitian, B. *Eur. J. Nucl. Med. Mol. Imaging* **2012**, *39*, 811.
53. Tang, D.; Hight, M. R.; McKinley, E. T.; Fu, A.; Buck, J. R.; Smith, R. A. Tantawy, M. N.; Peterson, T. E.; Colvin, D. C.; Ansari, M. S.; Nickels, M.; Manning, H. C. *J. Nucl. Med.* **2012**, *53*, 287.
54. Arlicot, N.; Vercouillie, J.; Ribeiro, M. J.; Tauber, C., Venel, Y.; Baulieu, J. L.; Maia, S.; Corcia, P., Stabin, M. G.; Reynolds, A.; Kassiou, M.; Guilloteau, D. *Nuc. Med. Biol.* **2012**, *39*, 570.
55. Abourbeh, G.; Thézé, B.; Maroy, R.; Dubois, A.; Brulon, V.; Fontyn, F.; Dollé, F.; Tavitian, B.; Boisgard, R. *J. Neurosci.* **2012**, *32*, 5728.

56. Lavisse, S.; Guillermier, M.; Hérard, A. S., Petit, F.; Delahaye, M.; Van Camp, N.; Ben Haim, L.; Lebon, V.; Remy, P.; Dollé, F.; Delzescaux, T.; Bonvento, G.; Hantraye, P.; Escartin, C. *J. Neurosci.* **2012***, 32*, 10809.

57. Kuhnast, B.; Damont, A.; Hinnen, F.; Catarina, T.; Demphel, S.; Le Helleix, S.; Coulon, C.; Goutal, S.; Gervais, P.; Dollé, F. *Appl. Rad. Isot.* **2012**, *70*, 489.

58. Corcia, P.; Tauber, C.; Vercoullie, J.; Arlicot, N.; Prunier, C.; Praline, J.; Nicolas, G.; Venel, Y.; Hommet, C.; Baulieu, J. L.; Cottier, J. P.; Roussel, C.; Kassiou, M.; Guilloteau, D.; Ribeiro, M. J. *PLoS One* **2012**, *7*, e52941.

59. Boutin, H.; Prenant, C.; Maroy, R.; Galea, J.; Greenhalgh, A. D.; Smigova, A.; Cawthorne, C.; Julyan, P.; Wilkinson, S. M.; Banister, S. D.; Brown, G.; Herholz, K.; Kassiou, M.; Rothwell, N. J. *PLoS One* **2013**, *8*, e56441.

60. Owen, D. R.; Howell, O. W.; Tang, S. P.; Wells, L. A.; Bennacef, I.; Bergström, M.; Gunn, R. N.; Rabiner, E.A.; Wilkins, M. R.; Reynolds, R.; Matthews, P. M.; Parker, C. A. *J. Cereb. Blood Flow Metab.* **2010**, *30*, 1608.

61. Owen, D. R.; Gunn, R. N.; Rabiner, E. A.; Bennacef, I.; Fujita, M.; Kreisl, W. C.; Innis, R. B.; Pike, V. W.; Reynolds, R.; Matthews, P. M.; Parker, C. A. *J. Nucl. Med.* **2011**, *52*, 24.

62. Owen, D. R.; Yeo, A. J.; Gunn, R. N.; Song, K.; Wadsworth, G.; Lewis, A.; Rhodes, C.; Pulford, D. J.; Bennacef, I.; Parker, C. A.; StJean, P. L.; Cardon, L. R.; Mooser, V. E.; Matthews, P. M.; Rabiner, E. A.; Rubio, J. P. *J. Cereb. Blood Flow Metab.* **2012**, *32*, 1.

63. Peyronneau, M. A.; Damont, A.; Valette, H.; Saba, W.; Delforge, J.; Goutal, S.; Bourgeois, S.; Hinnen, F.; Dollé, F.; Bottlaender, M. *J. Labelled Compd. Radiopharm.* **2009**, *52*, S385.

64. Peyronneau, M. A.; Saba, W.; Goutal, S.; Damont, A.; Dollé, F.; Kassiou, M.; Bottlaender, M.; Valette, H. *Drug Metab. Dispos.* **2013**, *41*, 122.

65. Damont, A.; Ching, A. S. C.; Médran-Navarrete, V.; Kuhnast, B.; Gaudy, H.; Dollé, F. *J. Labelled Compd. Radiopharm.* **2011**, *54*, S461.

66. Fernandez, M.-C.; Castaño, A.; Dominguez, E.; Escribano, A.; Jiang, D.; Jimenez, A.; Hong, E.; Hornback, W. J.; Nisenbaum, E. S.; Rankl, N.; Tromiczak, E.; Vaught, G.; Zarrinmayeh, H.; Zimmerman, D. M. *Bioorg. Med. Chem. Lett.* **2006**, *16*, 5057.

67. Spectroscopic data. Compound **7a**: ^{1}H-NMR ($CDCl_3$): δ 7.83 (d, 2H, J = 8.0 Hz), 7.55 (d, 2H, J = 8.0 Hz), 6.55 (s, 1H), 5.20 (d, 2H, J^2_{HF} = 47.6 Hz), 3.95 (s, 2H), 3.52 (q, 2H, J = 7.2 Hz), 3.40 (q, 2H, J = 7.2 Hz), 2.75 (s, 3H), 2.56 (s, 3H), 1.23 (t, 3H, J = 7.2 Hz), 1.11 (t, 3H, J = 7.2 Hz). ^{13}C-NMR ($CDCl_3$): δ 169.7 [C], 157.7 [C], 154.2 [C], 147.5 [C], 145.0 [C], 134.4 [C], 131.9 [2xCH], 128.5 [2xCH], 121.5 [d, J^4_{CF} = 4 Hz, C], 108.5 [CH], 101.4 [C], 89.5 [d, J^3_{CF} = 12 Hz, C], 83.2 [d, J^2_{CF} = 22 Hz, C], 71.1 [d, J^1_{CF} = 164 Hz, CH_2], 42.3 [CH_2], 40.6 [CH_2], 27.9 [CH_2], 24.4 [CH_3], 16.8 [CH_3], 14.3 [CH_3], 13.0 [CH_3]. Compound **7b**: ^{1}H-NMR ($CDCl_3$): δ 7.77 (d, 2H, J = 8.0 Hz), 7.48 (d, 2H, J = 8.0 Hz), 6.52 (s, 1H), 4.60 (dt, 2H, J^2_{HF} = 46.8 Hz, J^3_{HH} = 6.8 Hz), 3.94 (s, 2H), 3.50 (q, 2H, J = 7.2 Hz), 3.40 (q, 2H, J = 7.2 Hz), 2.86 (dt, 2H, J^3_{HF} = 19.2 Hz, J^3_{HH} = 6.8 Hz), 2.73 (s, 3H), 2.55 (s, 3H), 1.24 (t, 3H, J = 7.2 Hz), 1.11 (t, 3H, J = 7.2 Hz). ^{13}C-NMR ($CDCl_3$): δ 169.6 [C], 157.6 [C], 154.0 [C], 147.5 [C], 145.1 [C], 133.2 [C], 131.7 [2xCH], 128.5 [2xCH], 123.1 [C], 108.3 [CH], 101.3 [C], 89.4 [C], 85.1 [d, J^3_{CF} = 6 Hz, C], 81.3 [d, J^1_{CF} = 171 Hz, CH_2], 42.2 [CH_2], 40.6 [CH_2], 28.0 [CH_2], 24.1 [CH_3], 21.6 [d, J^2_{CF} = 24 Hz, CH_2], 16.9 [CH_3], 14.3 [CH_3], 13.0 [CH_3]. Compound **7c**: ^{1}H-NMR ($CDCl_3$): δ 7.76 (d, 2H, J = 8.0 Hz), 7.47 (d, 2H, J = 8.0 Hz), 6.54 (s, 1H), 4.62 (dt, 2H, J^2_{HF} = 47.2 Hz, J^3_{HH} = 6.0 Hz), 3.97 (s, 2H), 3.50 (q, 2H, J = 7.2 Hz), 3.41 (q, 2H, J = 7.2 Hz), 2.76 (s, 3H), 2.59 (t, 2H, J = 7.2 Hz), 2.58 (s, 3H), 2.01 (dq^5, 2H, J^3_{HF} = 25.6 Hz, J^3_{HH} = 6.0 Hz), 1.23 (t, 3H, J = 7.2 Hz), 1.12 (t, 3H, J = 7.2 Hz). ^{13}C-NMR ($CDCl_3$): δ 169.7 [C], 157.6 [C], 154.5 [C], 147.4 [C], 145.2 [C], 133.0 [C], 131.6 [2xCH], 128.4 [2xCH], 123.5 [C], 108.4 [CH], 101.3 [C], 89.3 [C], 82.5 [d, J^1_{CF} = 164 Hz, CH_2], 81.2 [C], 42.2 [CH_2], 40.6 [CH_2], 29.5 [d, J^2_{CF} = 20 Hz, CH_2], 28.0 [CH_2], 24.3 [CH_3], 16.9 [CH_3], 15.4 [d, J^3_{CF} = 4 Hz, CH_2], 14.3 [CH_3], 13.0 [CH_3]. Compound **7d**: ^{1}H-NMR ($CDCl_3$): δ 7.76 (d, 2H, J = 8.0 Hz), 7.46 (d, 2H, J = 8.0 Hz), 6.54 (s, 1H), 4.52 (dt, 2H, J^2_{HF} = 47.2 Hz, J^3_{HH} = 6.0 Hz), 3.96 (s, 2H), 3.50 (q, 2H, J = 7.2 Hz), 3.42 (q, 2H, J = 7.2 Hz), 2.75 (s, 3H), 2.58 (s, 3H), 2.50 (t, 2H, J = 7.2 Hz), 1.89 (m, 2H), 1.75 (q^5, 2H, J = 7.2 Hz), 1.20 (t, 3H, J = 7.2 Hz), 1.10 (t, 3H, J = 7.2 Hz). ^{13}C-NMR ($CDCl_3$): δ 169.6 [C], 157.6 [C], 154.9 [C], 147.5 [C], 146.0 [C], 132.7 [C], 131.6 [2xCH], 128.4 [2xCH], 123.8 [C], 108.3 [CH], 101.3 [C], 90.3 [C], 83.6 [d, J^1_{CF} = 164 Hz, CH_2], 81.1 [C], 42.2 [CH_2], 40.6 [CH_2], 29.5 [d, J^2_{CF} = 20 Hz, CH_2], 28.0 [CH_2], 24.4 [d, J^3_{CF} = 5 Hz, CH_2], 23.9 [CH_3], 19.1 [CH_2], 16.9 [CH_3], 14.2 [CH_3], 13.0 [CH_3].

68. *Determination of log$D_{7.4\,(HPLC)}$*. The retention time recorded for the tested compound was converted into its log$D_{7.4}$ value using a validated, standardized HPLC method (correlation between retention times and known logD values of similar compounds). HPLC conditions: Alliance 2695 - PDA Waters, X-Terra MS

C18 (4.6 x 20 mm, 3.5 µm) column ; mobile phase 5 mM MOPS / $(CH_3)_4NOH$ pH 7.4 (A), 5 % MOPS / $(CH_3)_4NOH$ (100 mM, pH 7.4) / 95 % CH_3CN (B) ; gradient (A / B): 98:2 (0.5 min), 0:100 (4.8 min), 98:2 (1.6 min) ; 1.2 mL/min ; 25 °C ; detection at 254 nm.

69. Peyronneau, M. A.; Saba, W.; Goutal, S.; Damont, A.; Dollé, F.; Kassiou, M.; Bottlaender, M.; Valette, H. *Drug Metab. Dispos.* **2013**, *41*, 122.
70. Dollé, F. *J. Labelled Compd. Radiopharm.* **2013**, *56*, 63.
71. Damont, A.; Roeda, D.; Dollé, F. *J. Labelled Compd. Radiopharm.* **2013**, *56*, 96.
72. Dollé, F.; Roeda, D.; Kuhnast, B.; Lasne, M.-C. In *Fluorine and Health: Molecular Imaging, Biomedical Materials and Pharmaceuticals*, Tressaud, A., Haufe, G., Eds.; Elsevier: Amsterdam, **2008**; pp 3-65.
73. Chauveau, F.; Van Camp, N.; Dollé, F.; Kuhnast, B.; Hinnen, F.; Damont, A.; Boutin, H.; James, M. L.; Kassiou, M.; Tavitian, B. *J. Nucl. Med.* **2009**, *50*, 468.

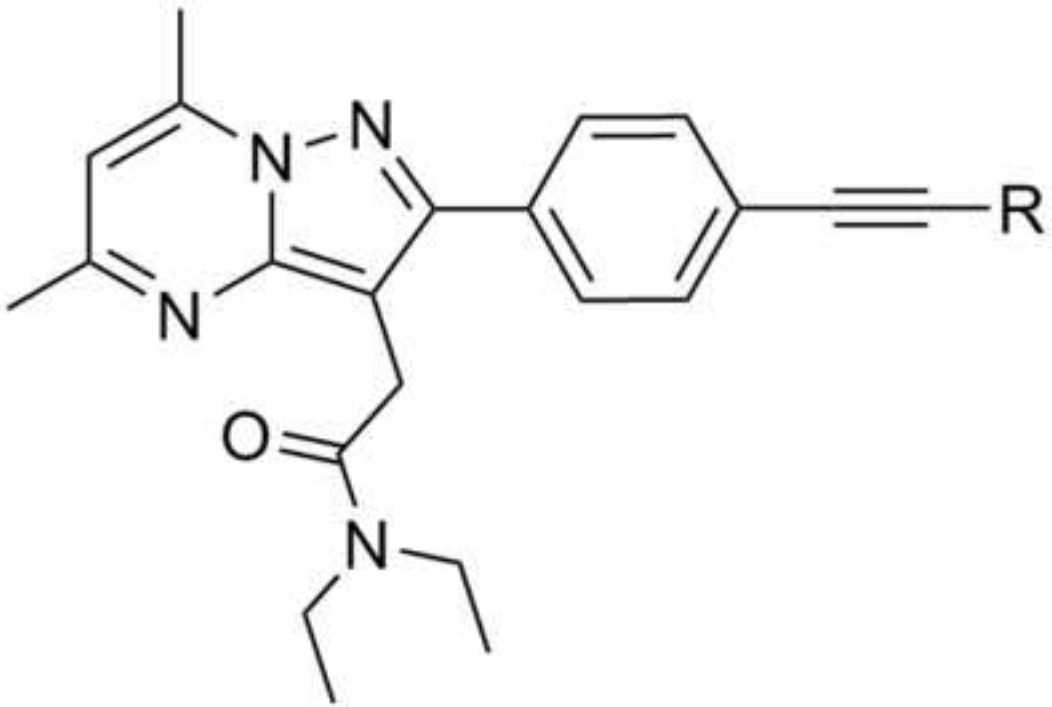

7a: R = CH_2F

7b: R = $(CH_2)_2F$

7c: R = $(CH_2)_3F$

7d: R = $(CH_2)_4F$

[^{18}F]-**7c**: R = $(CH_2)_3{}^{18}F$